UDK 669.24:544.022.822
Original scientific article/Izvirni znanstveni članek

ISSN 1580-2949
Mater. Tehnol.

GREEN AND CONVENTIONAL SYNTHESIS OF NiO NANOPARTICLES: IMPACT OF ERUCA SATIVA ON PHOTOCATALYSIS

ZELENA IN KONVENCIONALNA SINTEZA NANODELCEV NiO; VPLIV NAVADNE RUKVICE NA FOTOKATALIZO

Samia Remli[1*], Djanette Meriem Blizak[2], Salah Blizak[1,3]

[1]Research Unit Materials, Processes and Environment, M'hamed Bougara University, Boumerdes, Algeria
[2]Laboratory of Bioinformatics, Applied Microbiology and Biomolecules, University M'Hamed Bougara of Boumerdes, Boumerdes, Algeria
[3]Physics Department, University of M'sila, M'sila, Algeria

Prejem rokopisa – received: 2026-02-01; sprejem za objavo – accepted for publication: 2026-04-10

doi:10.17222/mit.2026.1659

In this study, we report a hybrid synthesis route to nickel oxide (NiO) nanoparticles that combines conventional sol–gel and Pechini methods with a green, bio-mediated approach using Eruca sativa (rocket) extract for the first time in NiO synthesis. This plant-based approach offers a genuinely sustainable alternative to purely chemical synthesis, while a factorial design helps us identify the specific contributions of each component. Four distinct samples were prepared from nickel acetate and calcined at 450 °C for two hours, then characterized by XRD, FTIR and UV–Vis spectroscopy to probe their structure and optical properties; their photocatalytic ability was evaluated by degrading methylene blue under UV light. Interestingly, the Pechini route produced markedly larger crystallites (41.3 nm) than the sol–gel co-precipitation method (15.5 nm), pointing to the decisive role of citric acid and ethylene glycol in steering crystal growth. More strikingly, incorporating rocket extract significantly narrowed the optical band gap – from 3.46 eV down to 3.22 eV in Pechini samples, and from 3.52 eV to 3.31 eV in the sol–gel batch. The best-performing catalyst was the bio-assisted Pechini sample, which degraded 65.6 % of the dye in 180 min, a clear improvement over the 43 % achieved by its conventional counterpart. Our findings suggest that blending optimized chemical routes with botanical extracts is a viable, powerful strategy for engineering high-efficiency NiO photocatalysts suited to sustainable water treatment.

Keywords: NiO nanoparticles, sol-gel, Pechini method, biosynthesis, Eruca sativa, photocatalysis

V članku avtorji poročajo o študiji hibridne poti sinteze nanodelcev nikljevega oksida (NiO), v kateri so združili običajni sol-gel postopek in Pechinijevo metodo z »zelenim«, biološko posredovanim preobratom. Pri tem so prvič uporabili ekstrakt rukole (navadna rukvica; lat.: Eruca sativa) za sintezo NiO. Avtorji povdarjajo, da ta rastlinski pristop ponuja resnično trajnostno alternativo izključno kemični sintezi, medtem ko je faktorska zasnova pomagala ločiti specifične prispevke posameznih komponent. Avtorji so pripravili štiri različne vzorce iz nikljevega acetata in njihovo dve urno kalcinacijo pri 450 °C. Nato so vzorce karakterizirali z XRD, FTIR in UV-Vis spektroskopijo, da bi raziskali njihovo strukturo in optične lastnosti. Njihovo fotokatalitsko sposobnost so ocenili na osnovi razgradnje metilensko modrega pod UV svetlobo. Zanimivo je, da je Pechinijeva pot ustvarila bistveno večje kristalite (41,3 nm) kot metoda sol-gel soprecipitacije (15,5 nm), kar kaže na odločilno vlogo citronske kisline in etilen glikola pri usmerjanju rasti kristalov. Še bolj presenetljivo je, da je vključitev ekstrakta rukole znatno zožila optično vrzel v pasu – s 3,46 eV na 3,22 eV v vzorcih Pechini in s 3,52 eV na 3,31 eV v sol-gel metodi. Izjemen rezultat je bil biološko podprti Pechinijev katalizator, ki je v 180 minutah razgradil 65,6 % barvila, kar je jasen skok v primerjavi s 43 %, ki jih je dosegel njegov konvencionalni ekvivalent. Ugotovitve avtorjev kažejo, da je mešanje optimiziranih kemijskih poti z botaničnimi ekstrakti izvedljiva in učinkovita strategija za inženiring visoko učinkovitih NiO fotokatalizatorjev, primernih za trajnostno čiščenje vode.

Ključne besede: NiO nanodelci, sol-gel metoda, Pechinijeva metoda, biosinteza, navadna rukvica ali rukola, fotokataliza

1 INTRODUCTION

Nanoscale metal oxides have experienced rapid growth in popularity in recent decades, thanks to their extraordinary physicochemical properties, which enable fascinating applications in catalysis, electronics, energy storage, and environmental remediation. Among them, nickel oxide (NiO), with its well-ordered cubic rocksalt structure, known as a wide-bandgap p-type semiconductor, stands out for its remarkable chemical and thermal robustness, not to mention its corrosion resistance, which makes it so versatile.[1] What is truly striking is its ability to adsorb, catalyse, and even use magnetic properties to trap both inorganic and organic pollutants in wastewater.[2] The mechanism by which these nanoparticles achieve remediation operates through a synergistic two-step process. In the first instance, the nanoparticles behave rather like molecular magnets, drawing in and adsorbing pollutants onto their surface. This initial adsorption phase establishes intimate contact between the pollutant and catalyst, which is essential for subsequent processes.[2] Once this contact has been established, the second phase begins. When NiO is excited by UV or visible light, electron-hole pairs are generated, which then produce highly

*Corresponding author's e-mail:
s.remli@univ-boumerdes.dz (Samia Remli)

reactive oxygen species (ROS) shortly thereafter. These include hydroxyl (OH) and superoxide (O_2^-) radicals, which are extraordinarily effective at oxidizing organic molecules at the molecular level. The effectiveness of this process has been well demonstrated with methylene blue, a pervasive industrial pollutant that is commonly encountered in textile effluents. Research has shown that its removal efficiency can reach as high as 97–99.6 % when conditions are properly optimized. Also, NiO achieves complete mineralization of these contaminants, breaking them down entirely into CO_2 and H_2O whilst keeping residual toxic waste to an absolute minimum.[3] This degradation capability highlights the potential of NiO as a sustainable solution for achieving clean water.

In reality, the photocatalytic efficiency of NiO depends on a delicate balance between several intrinsic parameters: crystallite size, specific surface area, particle morphology, and, of course, the presence of crystal defects. These factors are crucial because they directly control the recombination rate of photogenerated charges.[4] Several physical and chemical methods have been developed for the synthesis of metal oxide nanoparticles. Conventional chemical approaches such as hydrothermal synthesis, co-precipitation, and the sol-gel process have been explored by researchers for years. The conventional sol-gel process remains highly valued for its simplicity, low cost, and ability to produce homogeneous powders through direct hydrolysis and condensation of metallic precursors, thus forming a three-dimensional oxide network.[5] However, the Pechini method, conceived and patented by Mario P. Pechini in 1967, generally offers greater accuracy in terms of stoichiometry and crystalline purity. In stages, citric acid initiates the reaction by chelating the metal ligands, then ethylene glycol is added to trigger polyesterification, creating a complex polymer structure that blends the precursors down to the molecular level. The citric acid-glycol pairing keeps nucleation tidy and suppresses the formation of large aggregates, where plain sol-gel can end up with a real mishmash of particle sizes.[6]

The biosynthesis of NiO nanoparticles, particularly from plant sources, generally produces spherical or cubic morphologies ranging in size from 10 nm to 50 nm. The key difference lies in the substances present in various biological sources. These compounds act as natural engineers, serving as stabilizing and reducing agents that profoundly influence the initial formation of nanoparticles, their growth, crystallinity, and surface appearance.[7] This variation is clearly visible in research studies on NiO NPs biosynthesis: neem leaves, for example, produced regular cubic particles of approximately 10.5 nm,[8] while Indian almond leaves produced similar spherical particles of approximately 20 nm.[9] The secret lies in the plants themselves: their extracts are rich in secondary metabolites, such as polyphenols and flavonoids, which naturally adjust the size, shape, and surface characteristics of nanoparticles.[10] Even these plant-derived agents influence charge mobility and substance adhesion to the nanoparticles, demonstrating the complexity of structure and photocatalytic activity relationships. Jeyakumar et al. showed that 12.1 nm NiO NPs synthesized from Citrus medica leaf extract achieved an impressive 98 % degradation of methylene orange.[11] Rajith Kumar and colleagues achieved 98 % degradation of methylene blue under UV irradiation for 180 min, using 31 nm NiO NPs from Calotropis gigantea leaf extracts.[12] In another study,[13] olive leaf extracts (17 nm NiO NPs) achieved 95 % degradation of crystal violet under sunlight for only 40 min.

Eruca sativa, commonly known as rocket salad, is an aromatic plant that grows abundantly in the Mediterranean region. This plant is distinguished by its rich phytochemical composition. It contains significant amounts of flavonoids and sulphur compounds, which are largely responsible for its potent antioxidant activity.[14] Eruca sativa leaves are particularly rich in polyphenols and glucosinolates, biomolecules capable of interacting effectively with inorganic surfaces. To our knowledge, the use of Eruca sativa for the biosynthesis of NiO nanoparticles is reported here for the first time, offering an innovative, accessible, and environmentally friendly route for the production of these materials for environmental photocatalytic applications.

The main objective of this study is to evaluate the combined influence of the synthesis method and the preparation approach on the structural and photocatalytic properties of the NiO nanoparticles. The factorial design combines two chemical pathways (conventional sol-gel versus Pechini) and two modes of synthesis (chemical versus biosynthesis assisted by Eruca sativa extract) to analyse synergistic interactions and identify the optimal formulation for the photocatalytic degradation of methylene blue.

2 EXPERIMENTAL PART

2.1 Synthesis of the extract

The rocket (Eruca sativa) leaf extract used in this work was prepared as follows. Fresh aerial parts of the plant were collected from the Dellys region in Boumerdes, Algeria. The harvested rocket leaves were first washed carefully with water and then allowed to dry in the shade over a period of 72 h. After complete drying, the leaves were ground into a fine powder using a blender. For the extract preparation, 5 g of this powdered material was added to 100 mL of distilled water in a beaker. This mixture was subsequently heated to 50 °C whilst being stirred magnetically for one hour. Once the solution had cooled down to ambient temperature, it was filtered through Whatman No.1 filter paper to remove any solid residues. The resulting filtrate was collected and kept refrigerated at 4 °C until needed for the synthesis experiments (**Figure 1**).

Figure 1: Preparation of rocket extract

2.2 Synthesis of NiO nanoparticles

The Pechini polymeric route was adopted to synthesise Samples 1 (NiO NPs: Pechini) and 3 (NiO NPs: Pechini-Bio), in which 0.1 M nickel acetate tetrahydrate, $Ni(CH_3COO)_2{\cdot}4H_2O$, solution was heated to 80 °C and combined with citric acid and ethylene glycol. Upon adjusting the pH to 8 with ammonium hydroxide, a viscous greenish gel formed, which was dried at 120 °C to obtain a xerogel. In the case of the bio-assisted variation, Sample 3, the sole modification was the introduction of 50 mL of rocket extract during the initial dissolution phase. Both dried materials were subsequently ground and calcined at 450 °C for 2 h to crystallise the NiO.

By contrast, Samples 2 (NiO NPs: SG) and 4 (NiO NPs: SG-Bio) were prepared using the conventional sol-gel precipitation method. This involved heating the 0.1 M precursor solution and inducing precipitation by increasing the pH to 8 with sodium hydroxide. The resulting precipitates were subjected to centrifugation. They were thoroughly washed with a water-ethanol mixture. They were dried at 120 °C. In the case of the biological counterpart, Sample 4, the rocket extract was incorporated into the initial solution. Finally, both dried powders were calcined at 450 °C for two hours to produce the final oxide nanoparticles (**Figure 2**).

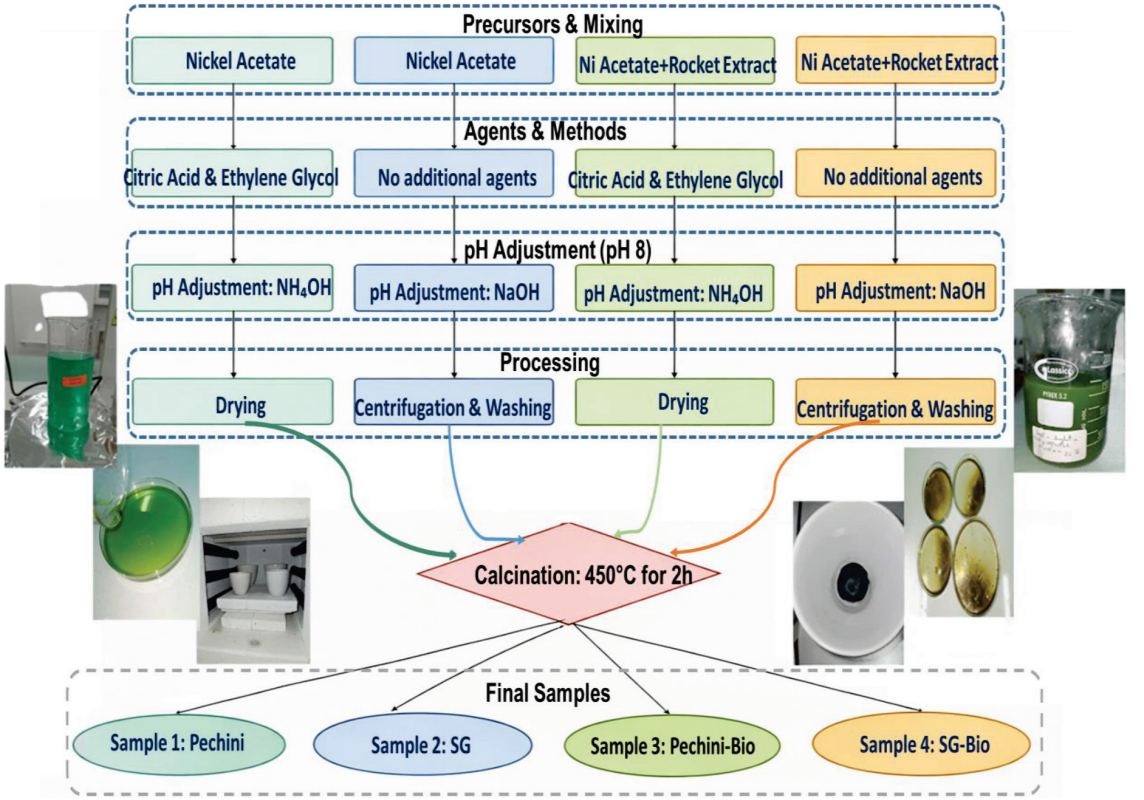

Figure 2: Preparation steps for the four NiO nanoparticle samples

3 RESULTS AND DISCUSSION

3.1 Crystalline phase and microstructural analysis (XRD)

We first determined the structure of the synthesized powders by X-ray diffraction (XRD). Figure 3 shows diffractograms of the four samples – Pechini, conventional sol-gel (SG) and their biosynthetic counterparts with Eruca sativa extract (Pechini-Bio and SG-Bio) – which confirm the formation of nickel oxide. The (111), (200), (220), (311) and (222) planes of the face-centred cubic (fcc) bunsenite phase of NiO (JCPDS 78-0643) are clearly identified by the characteristic peaks. As is frequently reported for nanocrystalline NiO,[12] the strong intensity of the (200) reflection together with the clear resolution of the characteristic diffraction peaks indicates good crystallinity of the synthesized nanoparticles. In addition, the absence of secondary diffraction peaks confirms the single-phase nature of the obtained NiO nanoparticles. The choice of the synthesis method had a significant impact on the size of crystallites. Sample 1 (NiO NPs: Pechini) exhibited an average crystallite size of 41.3 nm, whereas Sample 2 (the conventional sol-gel sample) showed a much smaller size of 15.5 nm (see **Table 1**). In this approach, citric acid acts as a chelating agent, generating stable metal-citrate complexes with Ni^{2+} ions.[15] During polymerisation with ethylene glycol, a polyester resin is formed. It is viscous and three-dimensional. This resin traps metal complexes in a rigid, homogeneous network. During calcination, this resin decomposes, but the process is highly controlled. The polymer matrix prevents premature aggregation of crystal nuclei and provides a confined environment for crystal growth. It reduces the number of nucleation sites while promoting the growth of those that do form.[16] This leads to fewer but larger crystallites. In contrast, the conventional sol-gel method relies on simple precipitation of $Ni(OH)_2$ after the addition of NaOH. This process is rapid and causes strong nucleation, resulting in the formation of a larger number of smaller crystallites, which have less opportunity for Ostwald ripening before being stabilised by calcination.[17] These findings align well with previous studies on metal oxide synthesis, where the Pechini method consistently provided larger and more uniform crystallites than conventional sol-gel approaches.[18]

The incorporation of Eruca sativa leaf extract during biosynthesis had an interesting moderating effect on crystallite size. The size of the crystallites in the Pechini pathway was reduced by almost 50 %: from 41.3 nm (NiO NPs; Pechini) to 20.6 nm (NiO NPs, Pechini-Bio). Similarly, using the conventional sol-gel method, the size decreased from 15.5 nm (NiO NPs; SG) to 11.2 nm (NiO NPs; SG-Bio). This trend, which is characteristic of green synthesis in the presence of plant extracts, was reported in numerous studies on the biosynthesis of metal oxide nanoparticles.[19,20]

The presence of the plant extract also led to notable changes in other structural parameters (see **Table 1**). The smallest particles (SG-Bio) had the highest microdeformation value (ε = 21.08 %) and the highest dislocation density ($\delta = 7.97 \times 10^{-3}$ lines/nm^2). Uddin et al. (2024) explain this observation by noting that smaller nanocrystals inherently have higher surface energy and undergo greater internal stresses due to their high surface-to-volume ratio. In addition, subtle disturbances in the crystal lattice can be induced by the incorporation of surface-adsorbed organic substances from a plant extract.[21] The potential of these structural defects as active sites for surface-dependent applications is a point to consider. In the case of photocatalysis, for example, improved catalytic performance is often the result of these defects, which provide additional reaction sites.[22]

3.2 UV–visible analysis

UV–visible spectroscopy studies of NiO nanoparticles demonstrate the profound effect that the synthesis method and incorporation of biological agents have on the material's optical properties. As can be seen in **Figure 4**, all of our samples exhibit strong absorption in the ultraviolet region. This corresponds to the characteristic band-to-band electronic transitions of nanocrystalline NiO. This behaviour of the wide-bandgap semiconductor is well documented.[23] However, it is clear that the absorption edge changes quite a lot from one sample to another. This is because there are differences in the size of the crystals, the amount of structural disorder, and the concentration of surface defects.

As shown in Figure 4, the analysis of Tauc plots, where $(\alpha h\nu)^2$ is plotted as a function of photon energy, confirm the direct band gap nature of NiO across the entire series, which is in agreement with the established data for NiO nanoparticles[24]. Numerically, the Pechini-derived NiO (D = 41.3 nm) exhibits a band gap of 3.46 eV, whereas the sol–gel sample, with its finer crys-

Table 1: Structural parameters obtained from the most intense peak (200) of NiO nanoparticles for the four samples

Sample	2θ (deg)	dhkl (nm)	Lattice parameter α (nm)	β (FWHM) (deg)	D (nm)	ε (%)	$\delta \times 10\text{^}15$ (lines/m^2)
Sample 1: NiO NPs (Pechini)	43.126	0.2096	0.4192	0.216000	41.3	5.76	0.586
Sample 2: NiO NPs (SG)	43.17	0.2094	0.4188	0.576000	15.5	15.35	4.162
Sample 3: NiO NPs (Pechini-Bio)	43.247	0.2091	0.4182	0.432000	20.6	11.48	2.365
Sample 4: NiO NPs (SG-Bio)	43.203	0.2093	0.4186	0.792000	11.2	21.08	7.97

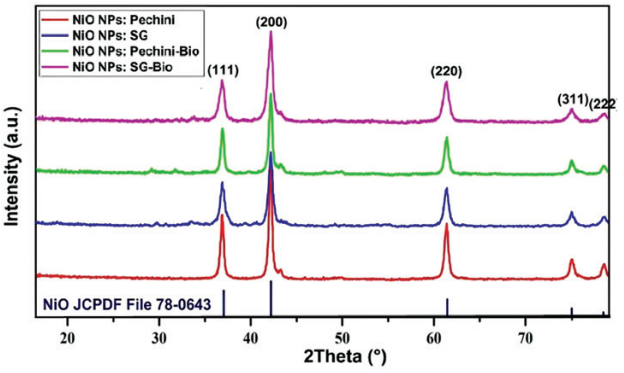

Figure 3: X-ray diffraction (XRD) spectra of the four samples: NiO NPs: Pechini; NiO NPs: SG; NiO NPs: Pechini-Bio; NiO NPs: SG-Bio

tallites (D = 15.5 nm), shows a clear widening to 3.53 eV. This phenomenon, whereby larger gaps are observed for smaller particles, reflects the quantum confinement effect, which is well documented for nanostructured metal oxides.[25] Yet the introduction of rocket extracts completely disrupts this pattern. Counter-intuitively, NiO-Pechini-Bio, despite larger crystallites (20.6 nm), displays a reduced gap of 3.22 eV, while NiO-SG-Bio, though much smaller (11.2 nm), reaches only 3.31 eV. This reversal finds its explanation in the specific chemistry at play. In the Pechini route, ethylene glycol acts not merely as a solvent but as a complexing agent that profoundly modifies defect formation. During calcination, this polyol generates a high concentration of oxygen vacancies, creating intermediate electronic states within the gap that effectively lower the optical transition energy.[26] In Pechini-Bio (rocket extract), this structural contribution overlaps with the surface modification induced by plant biomolecules with polyphenols and organic acids that alter the local dielectric environment.[27] The result is a synergistic reduction of the band gap that overrides the size effect. Conversely, the sol–gel route, lacking glycol, benefits only from the capping action of the biological extracts, yielding a more modest gap reduction (3.31 eV) despite the smaller crystallite size. These results are consistent with the data from Vijaya Kumar et al., who observed a similar reversal of the classical size-band gap hierarchy.[20] Their bio-synthesized NiO NPs (27 nm) in the presence of Gymnema sylvestre exhibit a band gap of 4.78 eV, compared to 5.1 eV for the chemically synthesized NPs (13 nm).

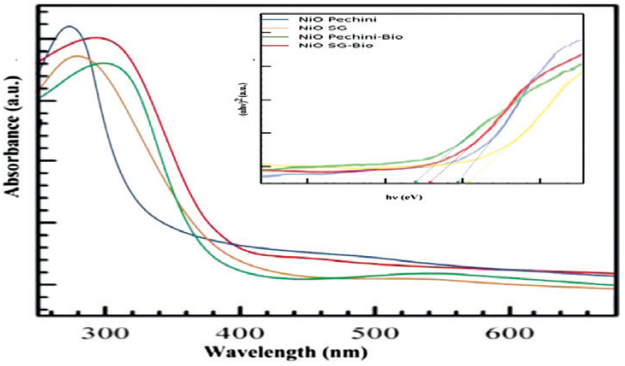

Figure 4: UV–Vis absorption spectra of the four samples: NiO NPs: Pechini, NiO NPs: SG, NiO NPs: Pechini-Bio, NiO NPs: SG-Bio

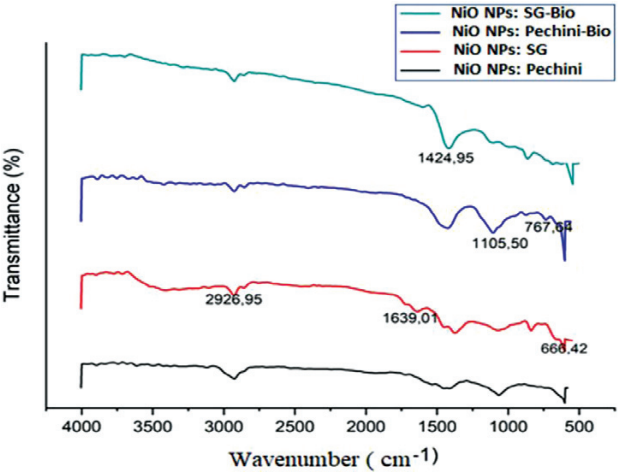

Figure 5: FTIR spectrum of the samples

3.3 FT-IR analysis

Our four samples were also analysed using a NICOLET iS70 FTIR transmittance spectrometer, for which KBr pellets were prepared by mixing the nanoparticle powder with potassium bromide. The infrared spectra obtained for the NiO powders are shown in **Figure 5**. The characteristic absorption band due to Ni–O bond vibrations is clearly visible in the 600–750 cm^{-1} region of the spectrum.[28] The width of this absorption band confirms that the NiO particles are indeed nanometric in size, which corroborates the previously mentioned X-ray diffraction results. The most consistent and significant observation is the persistence of the organic peaks (2926, 1425, 767 cm^{-1}) of the biosynthesized samples, even after calcination.[29] This result is crucial because it confirms that the phytochemical compounds in the Eruca sativa extract act as capping and stabilizing agents, forming a chemisorbed protective layer on the surface of the nanoparticles.[30]

3.4 Photocatalytic activity

The photocatalytic activity of nickel oxide (NiO) nanoparticles was evaluated by the degradation of Methylene blue (MB, $C_{16}H_{18}ClN_3S$) under UV irradiation. Because of its chemical stability, MB is frequently used as a model pollutant. The experiments were conducted in a reactor designed and built in our laboratory with an open enclosure lined with aluminum foil to maximize UV reflectance and a magnetic stirrer to ensure continuous homogenisation of the suspension. A 15 W UV lamp (JIA DI) was used as the irradiation source, and it was placed 15 cm above the reaction medium.

For every experiment, 50 mL of an aqueous MB solution containing 5 mg L^{-1} was mixed with 1 mg of NiO catalyst (catalyst loading: 20 mg L^{-1}). In order to establish adsorption–desorption equilibrium between the dye molecules and the catalyst surface, the suspension was kept in the dark under magnetic stirring for 30 minutes at room temperature prior to irradiation. The absorbance measured at the conclusion of this step was used as the initial value (A_0). After that, 180 minutes of UV radiation were applied. Aliquots of approximately 3 mL were withdrawn every 30 min, centrifuged at 6000 min^{-1} for 20 min to remove suspended NiO particles, and the resulting supernatant was analysed by UV–Vis spectrophotometry over a 500–700 nm range by monitoring the decrease of the characteristic MB absorption bands at 664 nm and 612 nm. The degradation percentage, D (%), was calculated as:

$$D(\%) = \frac{A_0 - A_t}{A_0} \times 100$$

where A_0 is the initial absorbance (after dark equilibrium) and A_t is the absorbance at time, t.

The temporal evolution of absorbance between 500 nm and 700 nm shows a steady decrease in the peaks at 664 nm and 612 nm, confirming a gradual disappearance of the dye under UV irradiation. The samples prepared by combining rocket extract with the Pechini or sol–gel methods degraded 65.6 % and 42.7 % of MB in 180 min (**Figure 5**), respectively, which is significantly higher than the performance obtained with conventional processes without rocket (> 20 %). This superiority can be explained by the microstructure induced by green synthesis: reduced crystallite size, increased specific surface area, and high density of oxygen vacancies that trap electrons, inhibit electron–hole recombination, and prolong the lifetime of charge carriers.[31] The catalyst concentration used (20 mg L^{-1}) is sufficient to generate an adequate number of active sites; at higher catalyst loadings, excess particles may induce a screening effect and reduce efficiency.[28] The organic residues in the extract also stabilize the surface and can act as sensitizers, enhancing energy transfer to the semiconductor.

The optical band gap plays an equally decisive part. In the bio-assisted samples, particularly NiO Pechini-Bio, the gap is narrowed to 3.22 eV (down from 3.46 eV in the conventional material), which pushes the absorption edge further into the visible range and allows charge carriers to form more readily under the UV lamp. These intermediate energy states act as electron traps that keep photogenerated holes and electrons apart, preventing rapid recombination.[3] By contrast, the NiO SG sample's wider gap of 3.52 eV demands higher-energy photons to excite electrons across the barrier, naturally limiting the fraction of incident light it can harness. Thus, the 'Pechini with rocket' pathway leads to a maximum photocatalytic activity of 65.6 %, demonstrating that de-

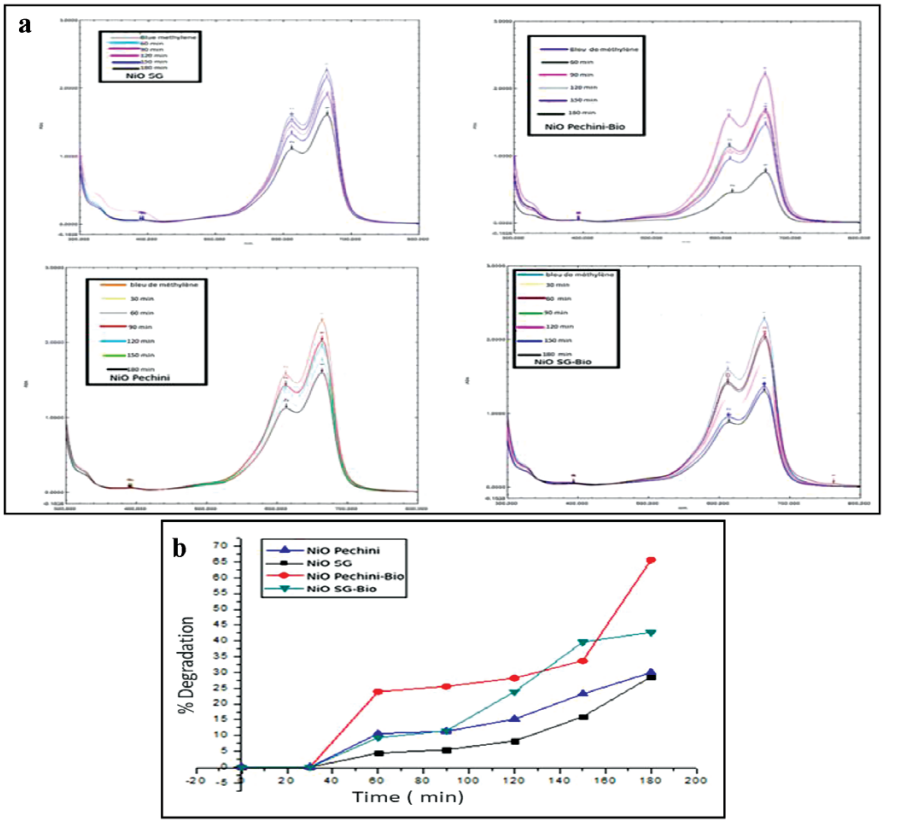

Figure 6: a) UV–visible absorption spectra of MB during photocatalytic degradation in the presence of NiO NPs; b) photodegradation efficiency of MB over different NiO catalysts

fect engineering through green synthesis is a relevant strategy for the removal of organic pollutants.[32,33]

5 CONCLUSIONS

This study reveals that combining conventional Pechini or sol–gel routes with Eruca sativa extract, a first for NiO NPs, yields surprising benefits that extend well beyond environmental credentials. Structurally, the Pechini method produced noticeably larger and more crystalline grains than the sol–gel approach, a difference rooted in the complexing action of citric acid and ethylene glycol during polymeric resin formation. Conversely, the sol–gel pathway generated finer, more dispersed particles. However, it was the plant extract that proved to be the real game-changer, systematically narrowing the optical band gap across both routes by creating oxygen vacancies and surface states. The bio-assisted Pechini sample exhibited the highest photocatalytic activity, with methylene blue being degraded far faster than by conventional counterparts. This improvement arises from three factors: the narrowed band gap enhances light absorption, while defects and increased surface area promote charge separation, enabling sufficient time for reactions to occur.

Green synthesis is not merely an environmentally friendly approach; it serves as a practical means of tuning crystal structure and electronic properties, offering a genuine pathway to efficient wastewater treatment.

6 REFERENCES

[1] S. S. Narender, V. V. S. Varma, C. S. Srikar, J. Ruchitha, P. A. Varma, B. V. S. Praveen, A brief review of the synthesis, characterization, and applications of nickel oxide nanoparticles, Chem. Eng. Technol., 45 (**2022**) 3, 397-409, doi:10.1002/ceat.202100442

[2] S. Thakur, I. Thakur, R. Kumar, A review on synthesized NiO nanoparticles and their utilization for environmental remediation, Inorg. Chem. Commun., 172 (**2025**), 113758, doi:10.1016/j.inoche.2024.113758

[3] I. Seete, D. A. Bopape, L. M. Mahlaule-Glory, Z. Tetana, N. C. Hintsho-Mbita, Plant-Mediated Synthesis of NiO Nanoparticles for Textile Dye Degradation in Water: A Review, Colorants, 4 (**2025**) 1, 7, doi:10.3390/colorants4010007

[4] M. J. Kadhim, M. A. Mahdi, A. M. Selman, A. A. S. K. Jamel, J. J. Hassan, N. M. Ahmed, The most important parameters that affect the photocatalytic activity of ZnO nanostructures against organic dyes: a review, (**2023**), doi:10.30495/ijc.2023.1969439.1966

[5] C. J. Brinker, G. W. Scherer, Sol-Gel Science: The Physics and Chemistry of Sol-Gel Processing, Gulf Prof. Publ., 1990

[6] K. I. Nassar, S. S. Teixeira, M. P. Graça, Sol–Gel-Synthesized Metal Oxide Nanostructures: Advancements and Prospects for Spintronic Applications—A Comprehensive Review, Gels, 11 (**2025**) 8, 657, doi:10.3390/gels11080657

[7] B.-A Miu, A. Dinischiotu, New Green Approaches in Nanoparticles Synthesis: An Overview, Molecules, 27 (**2022**) 19, 6472, doi:10.3390/molecules27196472

[8] L. Yadeta Gemachu, A. Lealem Birhanu, Green synthesis of ZnO, CuO and NiO nanoparticles using Neem leaf extract and comparing their photocatalytic activity under solar irradiation, Green Chem. Lett. Rev., 17 (**2024**) 1, doi:10.1080/17518253.2023.2293841

[9] M. M. Asai, K. Tapadia, Structure-function relationship of novel bio-inspired magnetic M-NiO nanoparticles with enhanced dye adsorption and antibacterial activity, Mater. Sci. Eng. B, 324 (**2026**), 118976, doi:10.1016/j.mseb.2025.118976

[10] C. P. Devatha, A. K. Thalla, S. Y. Katte, Green synthesis of iron nanoparticles using different leaf extracts for treatment of domestic waste water, J. Clean. Prod., 139 (**2016**), 1425–1435, doi:10.1016/j.jclepro.2016.09.019

[11] S. J. Jeyakumar, R. Piriyadharsini, M. Jothibas, Facile green synthesis of nickel oxide nanoparticles using Citrus medica leaf derivatives, characterization and study of dye degradation activity, Optik, 336 (**2025**), 172442, doi:10.1016/j.ijleo.2025.172442

[12] C. R. Kumar, V. S. Betageri, G. Nagaraju, G. H. Pujar, B. P. Suma, M. S. Latha, Photocatalytic, nitrite sensing and antibacterial studies of facile bio-synthesized nickel oxide nanoparticles, J. Sci. Adv. Mater. Dev., 5 (**2020**) 1, 48–55, doi:10.1016/j.jsamd.2020.02.002

[13] N. F. Alotaibi, A. H. Alanazi, S. M. Moustafa, M. F. Hasaneen, H. Bilel, R. Abdel-Hameed, A. M. Nassar, Photocatalysis and Biomedical Applications of Phytofabricated Nickel Oxide Nanoparticles via Olive Leaf Extract, Chem. Biodivers., (**2025**), e01963 doi:10.1002/cbdv.202501963

[14] A. M. Hazbar, A. M. N. Jassim, M. T. Mohammed, Y. Baqi, Biosynthesized Gold Nanoparticles from Eruca sativa Mill. Leaf Extract Exhibits In Vivo Biocompatibility, Antimicrobial, and Antioxidant Activities, Antibiotics, 14 (**2025**) 8, 776, doi:10.3390/antibiotics14080776

[15] M. Y. Nassar, I. S. Ahmed, I. Samir, A novel synthetic route for magnesium aluminate (MgAl2O4) nanoparticles using sol–gel auto combustion method and their photocatalytic properties, Spectrochim. Acta Part A: Mol. Biomol. Spectrosc., 131 (**2014**), 329–334, doi:10.1016/j.saa.2014.04.040

[16] S. Bayat, D. Ghanbari, M. Salavati-Niasari, Pechini synthesis of Co2SiO4 magnetic nanoparticles and its application in photo-degradation of azo dyes, J. Mol. Liq., 220 (**2016**), 223–231, doi:10.1016/j.molliq.2016.04.066

[17] D. Navas, S. Fuentes, A. Castro-Alvarez, E. Chavez-Angel, Review on sol-gel synthesis of perovskite and oxide nanomaterials, Gels, 7 (**2021**) 4, 275, doi:10.3390/gels7040275

[18] S. Dimesso, Pechini processes: an alternate approach of the sol-gel method, preparation, properties, and applications, In: Handbook of Sol-Gel Science and Technology, Springer, Cham. 2018, 1067–1088

[19] W. Ahmad, S. C. Bhatt, M. Verma, V. Kumar, H. Kim, A review on current trends in the green synthesis of nickel oxide nanoparticles, characterizations, and their applications, Environ. Nanotechnol. Monit. Manag., 18 (**2022**), 100674, doi:10.1016/j.enmm.2022.100674

[20] P. Vijaya Kumar, A. Jafar Ahamed, M. S. Karthikeyan, Synthesis and characterization of NiO nanoparticles by chemical as well as green routes and their comparisons with respect to cytotoxic effect and toxicity studies in microbial and MCF-7 cancer cell models, SN Appl. Sci., 1 (**2019**), 1083, doi:10.1007/s42452-019-1113-0

[21] P. Kurhade, S. Kodape, R. Choudhury, Overview on green synthesis of metallic nanoparticles, Chem. Pap., 75 (**2021**) 10, 5187–5222, doi:10.1007/s11696-021-01693-w

[22] J. Zhang, J. Li, The oxygen vacancy defect of ZnO/NiO nanomaterials improves photocatalytic performance and ammonia sensing performance, Nanomaterials, 12 (**2022**) 3, 433, doi:10.3390/nano12030433

[23] A. K. Atul, S. K. Srivastava, A. K. Gupta, N. Srivastava, Synthesis and Characterization of NiO Nanoparticles by Chemical Co-precipitation Method: An Easy and Cost-Effective Approach, Braz. J. Phys., 52 (**2022**) 2, doi:10.1007/s13538-021-01006-2

[24] M. El-Kemary, N. Nagy, I. El-Mehasseb, Nickel oxide nanoparticles: Synthesis and spectral studies of interactions with glucose, Mater. Sci. Semicond. Process., 16 (**2013**) 6, 1747–1752, doi:10.1016/j.mssp.2013.05.018

[25] W. J. Duan, S. H. Lu, Z. L. Wu, Y. S. Wang, Size effects on properties of NiO nanoparticles grown in alkalisalts, J. Phys. Chem. C, 116 (**2012**) 49, 26043–26051, doi:10.1021/jp308073c

[26] K. Pavithra, S. M. S. Kumar, Embedding oxygen vacancies at SnO2–CNT surfaces via a microwave polyol strategy towards effective electrocatalytic reduction of carbon-dioxide to formate, Catal. Sci. Technol., 10 (**2020**) 5, 1311–1322, doi:10.1039/C9CY01960J

[27] M. Mahmud, M. S. Rahman, A Concise Review on Applications of Nickel Oxide Nanoparticles and their Extraction Parts, Int. J. Adv. Biol. Biomed. Res., 13 (**2025**) 3, 317–340, doi:10.48309/IJABBR.2025.2042688.1546

[28] S. D. Khairnar, V. S. Shrivastava, Facile synthesis of nickel oxide nanoparticles for the degradation of Methylene blue and Rhodamine B dye: a comparative study, J. Taibah Univ. Sci., 13 (**2019**) 1, 1108–1118, doi:10.1080/16583655.2019.1686248

[29] O. S. Ali, D. E. AL-Mammar, Adsorption of the Color Pollutant onto NiO Nanoparticles Prepared by a New Green Method, Iraqi J. Sci., (**2024**), 1824–1838, doi:10.24996/ijs.2024.65.4.4

[30] F. Gul, Z. Ullah, J. Iqbal, B. A. Abbasi, S. Ali, S. Kanwal, T. Mahmood, Ecofriendly synthesis characterization and biological activities of Eruca sativa mediated silver oxide nanoparticles, Sci. Rep., 15 (**2025**) 1, 13466, doi:10.24996/ijs.2024.65.4.4

[31] F. Zhan, G. Wen, R. Li, C. Feng, Y. Liu, Y. Liu, P. La, A comprehensive review of oxygen vacancy modified photocatalysts: synthesis, characterization, and applications, Phys. Chem. Chem. Phys., 26 (**2024**) 15, 11182–11207, doi:10.1039/D3CP06126D

[32] F. Moradnia, S. T. Fardood, A. Zarei, S. Heidarzadeh, A. Ramazani, Green synthesis of nickel oxide nanoparticles using plant extracts: an overview of their antibacterial, catalytic, and photocatalytic efficiency in the degradation of organic pollutants, Iran. J. Catal., 14 (**2024**) 1, doi:10.57647/j.ijc.2024.1401.01

[33] S. Cui, G. Mu, Y. Li, J. Feng, F. Lu, F. Wang, L. Jia, Regenerating hazardous waste: enhancing photocatalytic performance through heterojunctions and oxygen vacancy-driven charge transport, Green Chem., 28 (**2026**), doi:10.1039/D5GC05333A